

Self-Organization of Ripples and Islands with SiGe-MBE

G. Chen, H. Lichtenberger, G. Bauer, and F. Schäffler

Institute of Semiconductor and Solid State Physics,
Johannes Kepler University, A-4040 Linz, Austria

We explored two methods to obtain laterally ordered Ge/Si quantum dot arrays. For the first we exploit the two independent growth instabilities of the SiGe/Si(001) hetero-system, namely kinetic step bunching and Stranski-Krastanov (SK) island growth, to implement a two-stage growth scheme for the fabrication of long-range ordered SiGe islands. The second approach is to deposit Ge/SiGe onto prepatterned Si substrates, which are prepared via lithography and subsequent reactive ion etching (RIE). It results in perfectly ordered, 2D dot arrays that can be extended into 3D by strain-ordering of a Ge-dot superlattice.

Introduction

The self-organized growth of Ge/Si quantum dot hetero-structures has attracted considerable interest because of its potential for electronic and optoelectronics devices, and its compatibility with the well-explored Si-technology. Recently, laterally ordered Ge/Si quantum dots have also been suggested for the implementation of quantum computing functions, as well as quantum information storage, which both require the separate identification and external addressability of each quantum dot. To obtain laterally ordered Ge/Si quantum dot arrays, we explored two methods. (i) A route which is only based on self-organization to achieve ordering is based on a slightly vicinal Si(001) surface, which is intrinsically unstable against kinetic-step-bunching during homoepitaxial growth. The resulting ripple morphology serves as a one-dimensional template for preferential Ge dot nucleation. (ii) Another approach is to deposit Ge/SiGe onto two-dimensionally prepatterned Si-substrates, which are prepared via lithography and subsequent reactive ion etching (RIE).

Results and Discussion

The Si(001) surface is intrinsically unstable against kinetic step bunching during Si homo- and SiGe heteroepitaxy [1] – [4]. This phenomenon was originally attributed to lattice-mismatch strain [5], but it is now clear that it is of purely kinetic origin. Recent kinetic Monte Carlo simulations in connection with a basic stability analysis provide strong evidence for step bunching being caused by the interplay between the adsorption/desorption kinetics at single atomic height steps and the pronounced diffusion anisotropy on the reconstructed Si(001) surface [6], [7]. The simulations show excellent agreement with STM experiments, and qualitatively reproduce the pronounced temperature dependence of the step bunching phenomena.

The detailed understanding of homoepitaxial step bunching on Si(001) allowed us to tailor the period and height of the bunches by controlling substrate miscut, growth temperature, deposition rate and layer thickness (Fig. 1). This way, homoepitaxial layers with ripple periods of 100 ± 10 nm were prepared on Si(001) substrates with 4° miscut along [110] (Fig. 2).

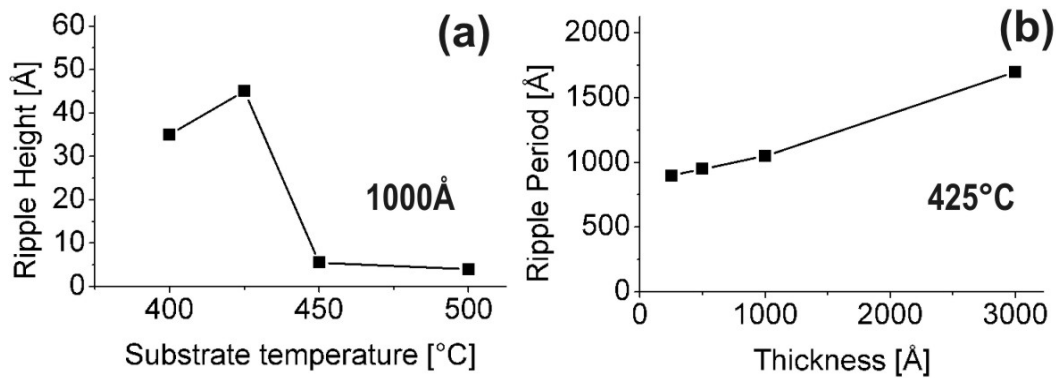


Fig. 1: (a) Dependence of the step-bunching ripple height on substrate temperature for a 1000Å Si-buffer. The maximum of the instability for 4° miscut and a Si-rate of 0.2Å/s occurs around 425°C; (b) Increase of the ripple period with thickness for the optimum Si-buffer temperature at 425°C.

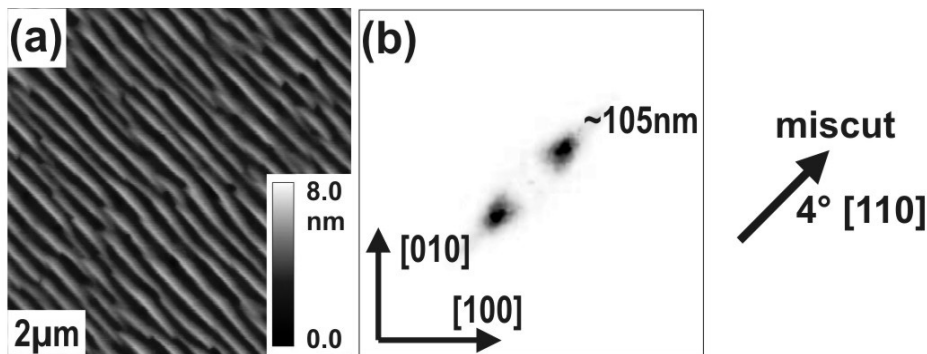


Fig. 2: (a) Kinetic step bunching of a homoepitaxial Si layer on a vicinal Si(001) substrate with 4° miscut along [110]. (b) Fast Fourier Transform showing a spacing for the step bunches of 100 ± 10 nm.

These were then employed as templates for the ordering of SiGe or Ge dots grown in the strain-driven Stranski-Krastanov mode. When the period length of the template complies with the mean spacing of the dots, only one dot row fits into one period (Fig. 3).

We could show that the dots then nucleate at the step bunches, where the energetically favorable $\{1\ 0\ 5\}$ facets of the dots are most easily created by step-meandering $[8] - [11]$. Considering growth further away from thermal equilibrium, the $\text{Si}_{0.55}\text{Ge}_{0.45}$ film deposited at 425 °C does not completely disintegrate into individual islands, but reveals how and where island nucleation commences: Upon SiGe deposition the flanks of the step bunches are converted into a zigzag train of adjacent $(1\ 0\ 5)$ and $(0\ 1\ 5)$ facets.

The originally smooth flanks match quite well the slope of the $[5\ 5\ 1]$ intersection line between two adjacent $\{1\ 0\ 5\}$ facets and thus can easily be converted into a $\{1\ 0\ 5\}$ faceted SiGe ridge structure, which is perpendicular to the step-bunches. This is a step-meandering instability induced by strain and the low-energy $\{1\ 0\ 5\}$ facets of SiGe on Si(001). It marks the transition (Fig. 4) from conformal Si/SiGe epilayer growth to strain-driven, ordered 3D-growth which is observed at 625°C for the $\text{Si}_{0.55}\text{Ge}_{0.45}$ epilayer. This leads to a fair degree of 2D rectangular, face-centered ordering of the SiGe dots (Fig. 3 (d)) in an approach that employs self-organization mechanisms only [9] – [12].

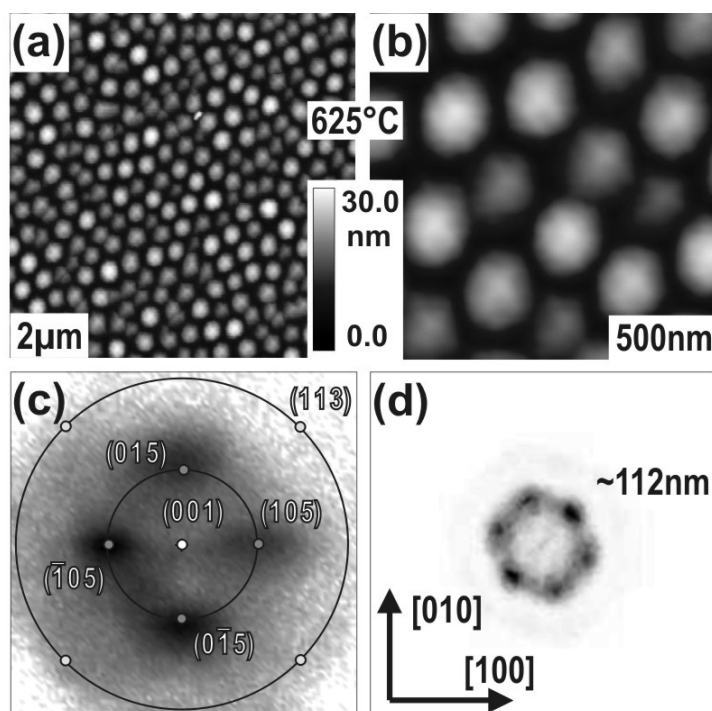


Fig. 3: (a), (b) Self-organized SiGe dots on the Si template from Fig. 2 with the 50 Å $\text{Si}_{0.55}\text{Ge}_{0.45}$ epilayer deposited @ 625°C; (c) Surface orientation maps derived from Fig. 2 (a). The dots show preferentially $\{1\ 0\ 5\}$ facets (inner circle). (d) Fast Fourier Transform of Fig. 3 (a), revealing rectangular, face-centered ordering of the dots.

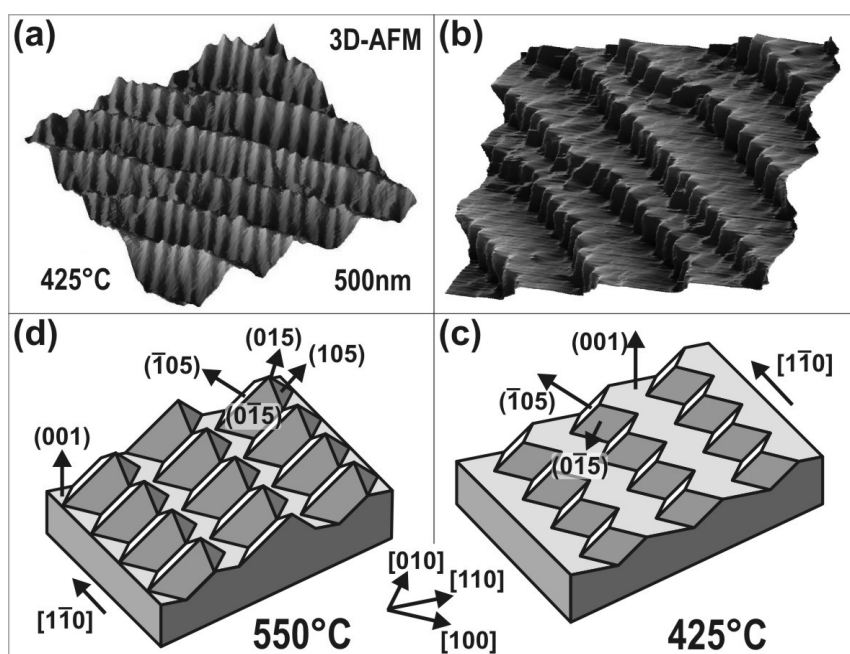


Fig. 4: (a), (b) 3D-AFM representations of a 50 Å $\text{Si}_{0.55}\text{Ge}_{0.45}$ -layer grown @ 425 °C showing a strain-induced $\{1\ 0\ 5\}$ zigzag structure decorating the bunch flanks. The dominant facets for SiGe layers deposited at 425 and 550 °C are depicted schematically in (c) and (d) respectively. At 550 °C also retrograde $\{1\ 0\ 5\}$ facets appear which are necessary to form 3D-islands as depicted in Fig. 3.

To realize perfectly ordered SiGe and Ge dots in 2D and 3D, we used lithographically defined pit arrays. For small enough periods, only one dot per unit cell is created, which nucleates at the lowest point of the pit (Fig. 5).

XTEM images reveal that the nucleation site is defined by the intersection of neighboring facets, which form during Si buffer layer deposition on the nano-structured templates [13]. Thus, by combining nano-structuring with self-organized growth, arbitrarily large areas of perfectly ordered 2D SiGe and Ge dot arrays can be implemented [14] – [16]. On this base we also realized perfect 3D Ge dot arrays by additionally exploiting the strain-driven vertical ordering of Ge dots in a Si/Ge dot super-lattice [17].

Lithographically defined ordering of SiGe and Ge dots fulfills an essential precondition for all but the most elemental applications of self-organized dots, namely their addressability. Vertical stacking of such arrays provides the option to use the topmost dot layer as a self-aligned mask for selective ion implantation.

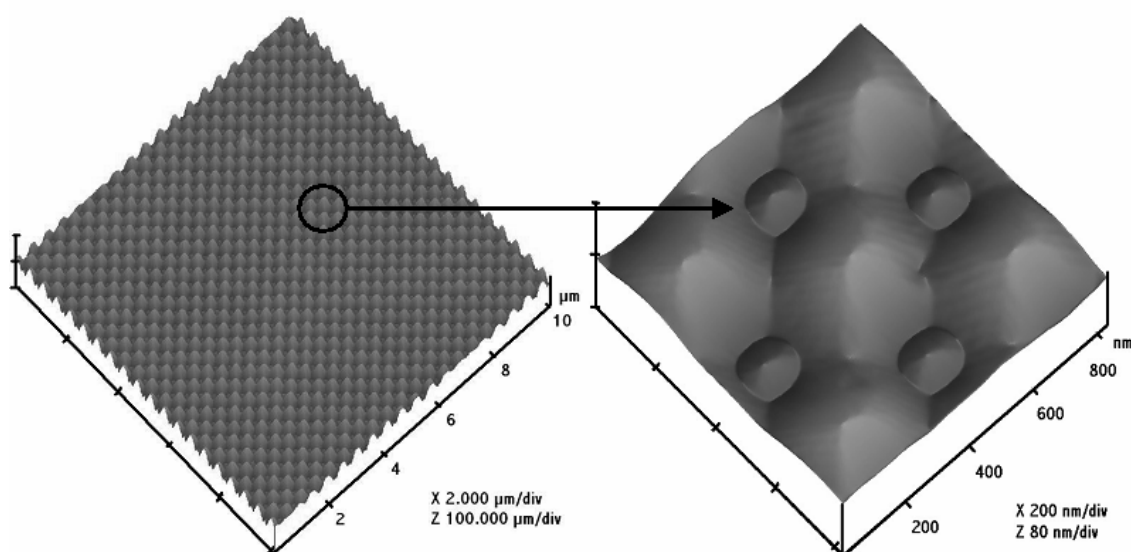


Fig. 5: 3D-AFM representations of a perfect 2D array of self-organized Ge with a periodicity of 350 nm on a Si template defined by lithography and reactive ion etching.

Acknowledgements

This work was supported by FWF P16223-N08 and INTAS 03-51-5015.

References

- [1] C. Schelling *et al* , *Phys. Rev. Lett.* **83**, 995 (1999).
- [2] C. Schelling *et al* , *Phys. Rev. B* **64**, 041301(R) (2001).
- [3] M. Mühlberger *et al* , *Surf. Sci.* **721**, 532 (2003).
- [4] A. Ronda *et al* , *Physica E* **23**, 370 (2004).
- [5] J. Tersoff *et al* , *Phys. Rev. Lett.* **75**, 2730 (1995).
- [6] J. Myslivecek *et al* , *Surf. Sci.* **520**, 193 (2002).
- [7] J. Myslivecek *et al* , *cond-mat/021231*.

- [8] H. Lichtenberger *et al* , *J. Cryst. Growth*, in print.
- [9] H. Lichtenberger *et al* , *Appl. Phys. Lett.* **86**, 131919 (2005)
- [10] C. Teichert *et al* , *Appl. Phys. A: Mater. Sci. Process.* **67**, 675 (1998).
- [11] J.-H. Zhu *et al* , *Appl. Phys. Lett.* **33**, 620 (1998).
- [12] C. Teichert *et al* , *Phys. Rep.* **365**, 335 (2002).
- [13] Z. Zhong *et al* , *J. Appl. Phys.* **93**, 6258 (2003).
- [14] Z. Zhong *et al* , *Appl. Phys. Lett.* **82**, 445 (2003).
- [15] Z. Zhong *et al* , *Appl. Phys. Lett.* **82**, 4779 (2003).
- [16] Z. Zhong *et al* , *Appl. Phys. Lett.* **83**, 3695 (2003).
- [17] Z. Zhong *et al* , *Physica E* **21**, 588 (2004).